IOP Publishing Smart Materials and Structures
Smart Mater. Struct. **30** (2021) 015017 (8pp) https://doi.org/10.1088/1361-665X/abcca2

Modelling ageing phenomenon in ferroelectrics via a Landau-type phenomenological model

Xuan He[1,3], Haoyuan Du[1], Dan Wang[2], Linxiang Wang[1] and Roderick Melnik[3,4]

[1] State Key Laboratory of Fluid Power and Mechatronic Systems, Zhejiang University, 310027 Hangzhou, People's Republic of China
[2] College of Mechanical and Electrical Engineering, Nanjing University of Aeronautics and Astronautics, Nanjing 210016, People's Republic of China
[3] MS2Discovery Interdisciplinary Research Institute, Wilfrid Laurier University, Waterloo ON N2L 3L5, Canada
[4] BCAM-Basque Center for Applied Mathematics, Alameda de Mazarredo 14, E-48009 Bilbao, Spain

E-mail: wanglx236@zju.edu.cn

Received 4 September 2020, revised 17 October 2020
Accepted for publication 20 November 2020
Published 9 December 2020

Abstract
In the current paper, the ageing and de-ageing phenomena in ferroelectric ceramics are modelled by a Landau-type model based on the internal bias field theory. A new phenomenological term for the internal bias electrical field is added into the free energy function to simulate the phenomenon of lattice symmetry during the ageing phenomenon. The simulations for both ageing and de-ageing phenomena are successfully presented in the current paper. The hysteretic behaviours of the ageing and de-ageing phenomena are captured very well by the proposed model.

Keywords: ferroelectrics, hysteresis loops, ageing, Landau theory, internal bias field

(Some figures may appear in colour only in the online journal)

1. Introduction

With more and more research and applications being developed for ferroelectric thin films in recent years, ageing and fatigue phenomena have also received more attention because the effects of ageing and fatigue phenomena in ferroelectric thin films are more obvious [1, 2]. Ageing phenomenon and fatigue phenomenon are both important factors that cause the polarization value of ferroelectric devices to decrease. The ageing phenomenon is also an important time-dependent phenomenon. Unlike fatigue, the polarization value decreases without any external load [3]. After ageing phenomenon, ferroelectrics usually exhibit an abnormal dual-polarization or contraction-polarized electric field hysteresis curve. Due to the above phenomenon, ageing can seriously affect the practical application of ferroelectrics, especially the reliability and stability of ferroelectric equipment. Generally, the ageing phenomenon leads to a decrease in the ferroelectric, dielectric, and piezoelectric properties of the ferroelectric, which is a harmful phenomenon. However, some studies have shown that due to the reversible domain flip mechanism, ageing can also produce a large recoverable electrical strain effect [4], and this effect is controllable and can improve the electromechanical performance of ferroelectric devices indirectly. Therefore, ferroelectric ageing is both a basic problem and a practical problem, and thus, it has attracted widespread attention in recent decades.

Regarding the causes of ageing phenomena, a large number of theoretical models have been proposed, such as the domain wall pinning model, volume effect model, etc. At present, there are still controversies about these models, but generally speaking, ageing phenomena can be attributed to material impurities or lattice defects. In the domain wall pinning model, material defects migrate to the domain wall during ageing, and, therefore, pin the domain wall to form a pinning effect [5, 6]. The volume effect model is based on the principle of symmetry

and consistency of point defects. In this model, polar defects will be arranged along the spontaneous polarization direction over the entire domain during ageing, so that the entire domain becomes stable and difficult to switch [7]. What all these mechanisms have in common is that there is an internal bias field in an aged sample. The internal bias field serves as an additional coercive field for correcting alignment defects [2]. The internal bias field will move or retract the hysteresis curve of the ferroelectric along the crystal axis. When material defects appear in the material, the hysteresis curve will be rearranged. At this time, the hysteresis curve will shrink and the phenomenon of double hysteresis can occur. In addition, this internal bias field usually shows a quasi-linear upward trend on a logarithmic time scale [8].

Although the domain wall pinning model and the volume effect mode have different views for the mechanism of ageing, they both simulate point defects to simulate the ageing phenomenon in their numerical simulations. Traditional models of this type simulate the phenomenon of point defects and dipoles through first-principles calculation [9, 10], which is very complicated in calculation. Another way to study the ageing model is to construct a continuum model using the phase-field method and then solve it with a finite element model [11, 12]. This method is simpler than the previous methods, but it is still relatively complicated for industrial control. The most suitable method for engineering control is to use phenomenological models, but the traditional phenomenological model cannot solve similar problems. Therefore, it is very meaningful to propose a phenomenological model that can simulate the ageing phenomenon. In response to the abovementioned problems, a phenomenological model based on Landau's theory combined with internal bias field theory was proposed to simulate the above phenomenon to facilitate engineering application control. In the current paper, a brief introduction to the ageing phenomenon and free energy function, as well as the governing equations of the ferroelectric ceramics is given. Both ageing and de-ageing phenomena are simulated with a detailed algorithm will be present in the 'Numerical experiment' section. Concluding remarks are given in the 'Conclusion' section.

2. Ageing phenomenon and free energy function

The process of the ageing phenomenon is shown in figure 1, and figure 1(a) shows the hysteresis curve for the ferroelectric in the original state. After the ageing process, due to the reasons discussed in the previous section, an internal biased electrical field is formed inside the ferroelectric ceramic, as shown in figure 1(b). At this time, the internal biased field makes the hysteresis curve shift towards the crystal axis. However, the state in Figure b is unstable and will not exist for a long time. After that, the hysteresis curve will gradually shrink and reach an equilibrium state, as shown in figure 1(c). This is the reason for the formation of the double hysteresis loop in the ageing phenomenon. The relationship between the polarization value measured in the final experiment and the external electric field is shown in figure 1(d).

To simplify the calculation of the model and facilitate the application of engineering control, the current paper selects a quasi-one-dimensional situation for modelling. In the current model, there are three polarization orientations (two 180° switching orientations and one non 180° switching orientation), which can be considered as a quasi-one-dimensional situation. This can be modelled by the Landau free energy function as follows [13]:

$$F_{\mathrm{L}}(P) = \frac{\mathrm{a}_2}{2}P^2 + \frac{\mathrm{a}_4}{4}P^4 + \frac{\mathrm{a}_6}{6}P^6, \tag{1}$$

where P is the polarization; $\mathrm{a}_2, \mathrm{a}_4$, and a_6 are the Landau coefficients. According to former publications [13–17], the free energy function and Rayleigh disspation termof ferroelectrics are chosen as follows:

$$\begin{aligned} \Psi(P,\varepsilon) &= F_L(P) + \frac{\mathrm{k}}{2}\varepsilon^2 + \frac{\mathrm{b}}{2}\varepsilon P^2 - EP - \varepsilon\sigma, \\ R &= \frac{1}{2}\tau_{\mathrm{p}}\left(\frac{\mathrm{d}P}{\mathrm{d}t}\right)^2 + \frac{1}{2}\tau_{\varepsilon}\left(\frac{\mathrm{d}\varepsilon}{\mathrm{d}t}\right)^2 \end{aligned} \tag{2}$$

where ε is the strain; b and k are the model constant; τ_{p} and τ_{ε} terms represent the damping effects.

However, merely using the free energy function in equation (2) cannot satisfy the simulation of ageing phenomena, and it cannot fully explain the changes in the lattice structure of b–c in the figure. To accomplish this goal and considering the symmetry of the lattice, a new item for the internal bias field $-E_{\mathrm{internal}}|\mathrm{P}|$ is considered to adjust the free energy function:

$$\Psi(P,\varepsilon) = F_{\mathrm{L}}(P) + \frac{\mathrm{k}}{2}\varepsilon^2 + \frac{\mathrm{b}}{2}\varepsilon P^2 - EP - \varepsilon\sigma - E_{\mathrm{internal}}|\mathrm{P}|. \tag{3}$$

With the help of new additional items, this model can easily complete the evolution from a single hysteresis loop to a double hysteresis loop, which is the part shown in figures 1(b)–(c). It is worth noting that this new additional item is phenomenological and is used to express the lattice reconstruction in the direction of the internal bias field. The following figure 2 describes the changes in the new additional terms for the hysteresis loops, which are sketched by the current model.

3. Governing equation

The governing equations for simulating ferroelectric single crystals can be obtained by applying the Euler–Lagrange equation to the free energy function in equation (3) and Rayleigh disspation term in equation (2):

$$\tau_p\frac{\mathrm{d}P}{\mathrm{d}t} + \mathrm{a}_2P + \mathrm{a}_4P^3 + \mathrm{a}_6P^5 + \mathrm{b}\varepsilon P - E - E_{\mathrm{internal}}\mathrm{sgn}(P) = 0, \tag{4}$$

$$\tau_{\varepsilon}\frac{\mathrm{d}\varepsilon}{\mathrm{d}t} + \mathrm{k}\varepsilon + \frac{1}{2}\mathrm{b}P^2 - \sigma = 0. \tag{5}$$

Each single crystal is connected to ceramics through the angle θ between the external electrical field and its crystal principal axis [16, 17].

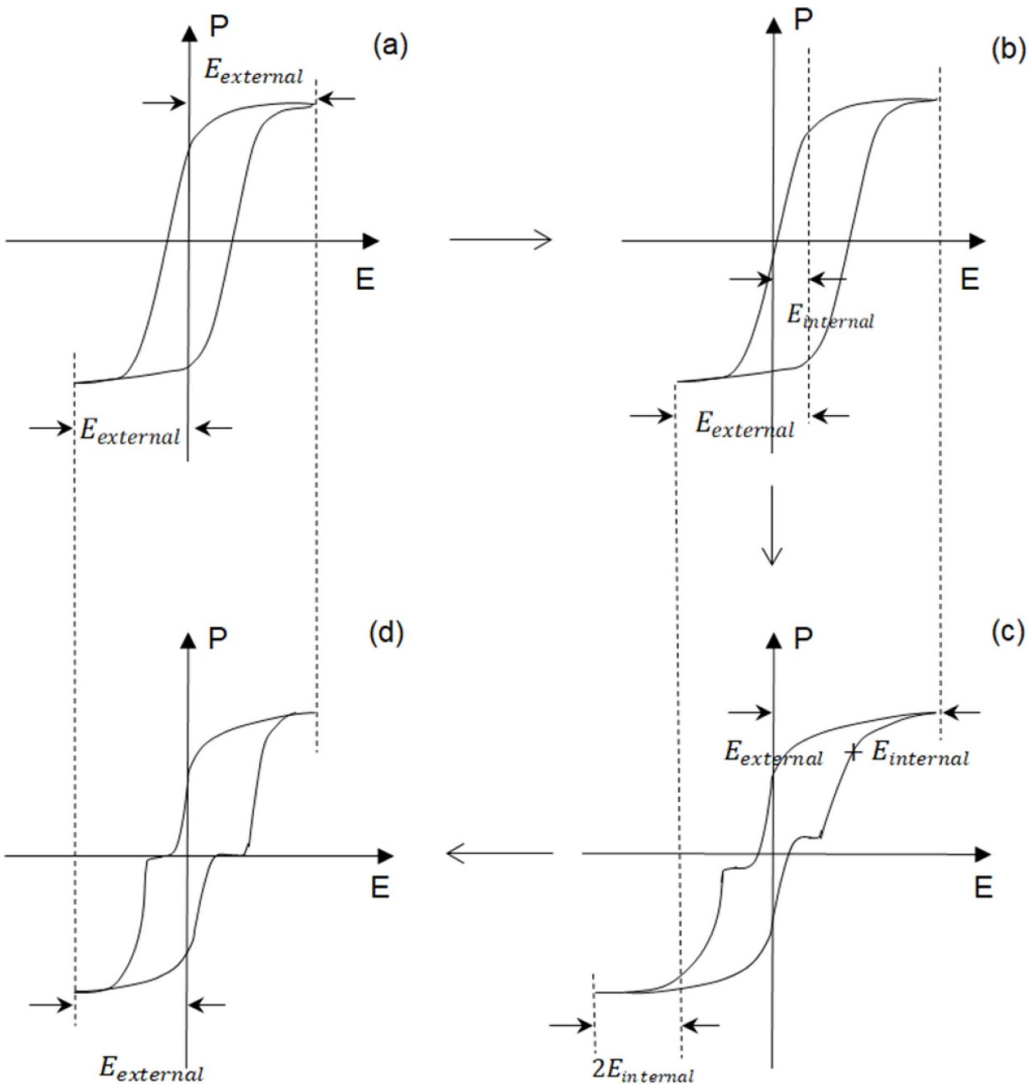

Figure 1. The theory of ageing phenomenon explained by internal bias electrical field theory. (a) The fresh ceramic; (b) Internal bias field appearing in an ageing ceramic; (c) Actual hysteresis loop after lattice evolution; (d) Measured hysteresis loop after lattice evolution.

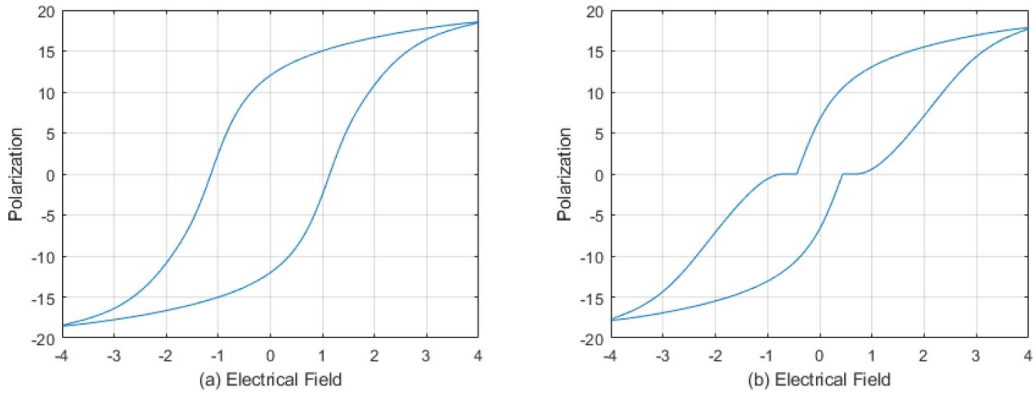

Figure 2. (a) Hysteresis loop without new term; (b) Hysteresis loop with new term.

$$\tau_{\mathrm{p}}\frac{\mathrm{d}P_\theta}{\mathrm{d}t}+\mathrm{a}_2P_\theta+\mathrm{a}_4{P_\theta}^3+\mathrm{a}_6{P_\theta}^5+\mathrm{b}\varepsilon_\theta P_\theta-\mathrm{E}\cos\theta-E_{\mathrm{internal}}\mathrm{sgn}\left(P\right)\cos\theta=0, \tag{6}$$

$$\tau_\varepsilon\frac{\mathrm{d}\varepsilon_\theta}{\mathrm{d}t}+\mathrm{k}\varepsilon_\theta+\frac{1}{2}\mathrm{b}{P_\theta}^2-\sigma\cos\theta=0. \tag{7}$$

The governing equations for simulating ferroelectric ceramics can be regarded as a combination of the governing equations for each single-crystal domain [17]:

$$P=\sum_{i=1}^{M}P_{\theta_i}W_i, \tag{8}$$

$$\varepsilon=\sum_{i=1}^{M}\varepsilon_{\theta_i}W_i, \tag{9}$$

where W_i is the weight function, which needs to be identified, of ith single crystal.

The quasi-one-dimensional model is a simplification of the actual three-dimensional (3D) situation. Therefore, the variable internal bias field in this article is merely a projection of the real variable in the 1D measurement direction. Since the actual situation is 3D, there will be some errors in the simulation. The error affected by non-180° domain switching is difficult to express directly in this model. Therefore, the current paper additionally sets the non-180° switching percentage as a new variable $\xi(t)$ to control the polarization loss caused by non-180°switching. Since the non-180°switching is directly related to the generation of the internal bias field, this article assumes that the value of $\xi(t)$ is positively related to the internal bias field. The new governing equations with variable $\xi(t)$ can be expressed as follows:

$$\tau_{\mathrm{p}}\frac{\mathrm{d}P_{\theta_i\xi}}{\mathrm{d}t}+\mathrm{a}_2P_{\theta_i\xi}+\mathrm{a}_4{P_{\theta_i\xi}}^3+\mathrm{a}_6{P_{\theta_i\xi}}^5+\mathrm{b}\varepsilon_{\theta_i}P_{\theta_i\xi}-\mathrm{E}\cos\theta-E_{\mathrm{internal}}\mathrm{sgn}\left(P_{\theta_i\xi}\right)\cos\theta=0, \tag{10}$$

$$\tau_\varepsilon\frac{\mathrm{d}\varepsilon_{\theta_i}}{\mathrm{d}t}+\mathrm{k}\varepsilon_{\theta_i}+\frac{1}{2}\mathrm{b}{P_{\theta_i\xi}}^2-\sigma\cos\theta=0, \tag{11}$$

$$P_{\theta_i\xi}=P_{\theta_i}/\left(1-\xi\left(t\right)\right). \tag{12}$$

$$\varepsilon_{\theta_i\xi}=\varepsilon_{\theta_i}/\left(1-\xi\left(t\right)\right). \tag{13}$$

$$P=\sum_{i=1}^{M}P_{\theta_i\xi}W_i, \tag{14}$$

$$\varepsilon=\sum_{i=1}^{M}\varepsilon_{\theta_i\xi}W_i. \tag{15}$$

4. Numerical experiment

The current research experiments on the ageing mechanism are mainly divided into ageing experiments and de-ageing experiments, so the simulations in this section are also divided into two parts, the first part is the ageing simulation, and the second part is the de-ageing simulation. The density function W_i is assumed as follows [17]:

$$\mathrm{W}_i=\alpha\mathrm{e}^{-\left[\frac{\ln\left(\theta_i/\gamma\right)}{\beta}\right]^2}, \tag{16}$$

where α, β, and γ are identified by the following simulations in this section. The optimization strategy for the final parameters is formed as a least square optimization problem [16]:

$$\min\ G=\sum_{i=1}^{N}\left(\left(\frac{\widetilde{P}_i-P_i}{P_{\mathrm{magnitude}}}\right)^2+\left(\frac{\widetilde{\varepsilon}_i-\varepsilon_i}{\varepsilon_{\mathrm{magnitude}}}\right)^2\right), \tag{17}$$

$\widetilde{P}_i$ and $\widetilde{\varepsilon}_i$ are the measurement values of the ith domain, P_i and ε_i are the simulated values of the ith domain, and $P_{\mathrm{magnitude}}$ and $\varepsilon_{\mathrm{magnitude}}$ are the magnitudes of the measurement data, which are applied here to obtain the relative errors. G is the value of the objective function, which needs to be optimized. The Runge-Kutta 45 method is used to compensate for the ordinary differential equations presented in the current paper.

4.1. Simulation of ageing phenomenon

The experimental data used in this section was obtained for KNN-1Mn ceramics from [18]. It should be noted here that, according to the research of Feng *et al*, the lattice structure has little effect on the principle of the ageing process, so different lattice structures can be simulated by the current model. According to the research described in [8], the internal bias field usually increases quasi-linearly on a logarithmic time scale, so we assume that the relationship between the internal bias field and time can be expressed as follows:

$$E_{\mathrm{internal}}\left(t\right)=m+A\log\left(\frac{t}{t_0}\right). \tag{18}$$

However, because the ageing process in [18] is too complicated and lacks sufficient data, the experiments in this part can only be simplified to two points: fresh sample and aged sample. Therefore, only the internal bias field and $\xi(t)$ of the aged sample will be identified instead of equation (18). According to the experimental data, there is the residual strain in this simulation, so the total strain is rewritten as follows:

$$\varepsilon_{\mathrm{total}}=\varepsilon+\varepsilon_{\mathrm{Residual}}. \tag{19}$$

A detailed strategy for parameter identification is presented as follows:

(a) Identify the initial values for the single-crystal model parameters τ_p, a_2, a_4, a_6, τ_ε, k and b by using the fresh sample data; (this step can be referred to former publications [19])

Table 1. Parameter values in the ageing simulation.

Parameters	Initial value	Optimized value
τ_p	0.00026415	0.00026415
a_2	−0.12830	−0.12833
a_4	0.0013955	0.0013959
a_6	0.0000026104	0.0000028804
τ_ε	7.0377	7.6290
b	−4.7586	−5.8461
k	4610.2	8232.1
σ_{bias}	−300.00	−333.25
$E_{\text{internal}}\,(\text{aged})$	0.50000	0.65961
$\xi\,(aged)$	1.0000	0.97001
$\varepsilon_{\text{Residual}}$	0.0000	0.039461
W_i	$1.0000\text{e}^{-\left[\frac{\ln(\theta_i/0.00010000)}{4.0000}\right]^2}$	$0.91751\text{e}^{-\left[\frac{\ln(\theta_i/0.000088551)}{3.8523}\right]^2}$

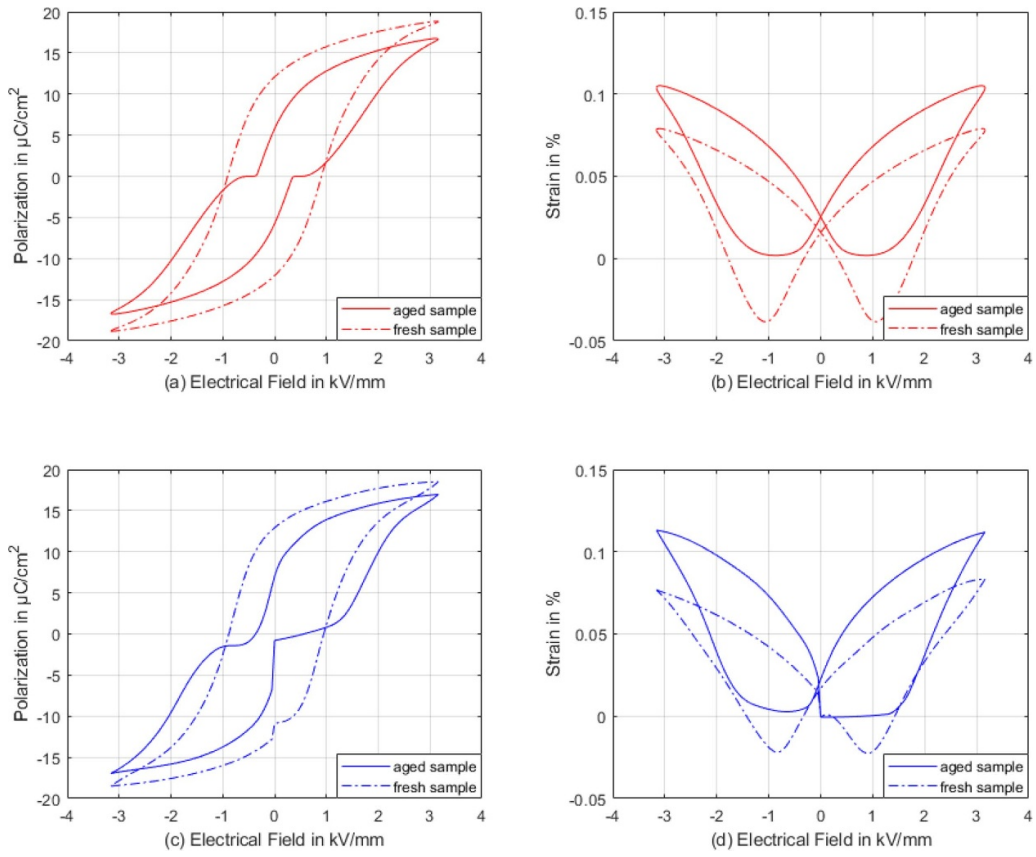

Figure 3. Hysteresis loops in the ageing simulation: (a) simulation value for polarization; (b) simulation value for strain; (c) measured polarization value; (d) measured strain value.

(b) Identify the initial values of the internal bias field variable $E_{\text{internal}}\,(t)$, residual strain $\varepsilon_{\text{Residual}}$ and non-180° switching percentage variable $\xi\,(t)$ by using the aged sample data;
(c) Complete the single-crystal optimization problems with the initial values obtained from step 1–2;
(d) Determine the initial value of the density function α, β, and γ through the initial value of each single crystal model in step 3;
(e) Identify the final parameter values with the initial values obtained above using the strategy in equation (17).

All the values in this part can be referred to table 1 and the hysteresis loops can be seen in figure 3. Figures 3(a) and (c) are the hysteresis loops for the simulation and measured polarization values, respectively. Figures 3(b) and (d) are the 'butterfly' loops of the simulation and the measured strain values, respectively. The effect of new additional items on ageing simulation is significant. However, since the above process only describes the two-point state, it is not enough to demonstrate the time-dependent simulation ability of the current model. Thus, the time-dependent process can be considered in the

Table 2. Parameter values in the de-ageing simulation.

Parameters	Initial value	Optimized value
τ_p	56.252	44.840
a_2	4.2843	4.5026
a_4	−96.585	−86.832
a_6	934.89	773.51
τ_ε	0.000053954	0.000077219
b	−0.0064758	−0.0056371
k	0.0016785	0.0019583
$E_{\text{internal}}(t)$	$0.51492e^{-\frac{t}{11.096}} + 0.00065914$	$0.49553e^{-\frac{t}{11.502}} + 0.00060930$
$\xi(t)$	$0.20401e^{-\frac{t}{22.439}} + 0.000046133$	$0.20362e^{-\frac{t}{21.563}} + 0.000049175$
W_i	$0.38680e^{-\left[\frac{\ln(\theta_i/0.00012032)}{4.2755}\right]^2}$	$0.24036e^{-\left[\frac{\ln(\theta_i/0.000038921)}{5.2045}\right]^2}$

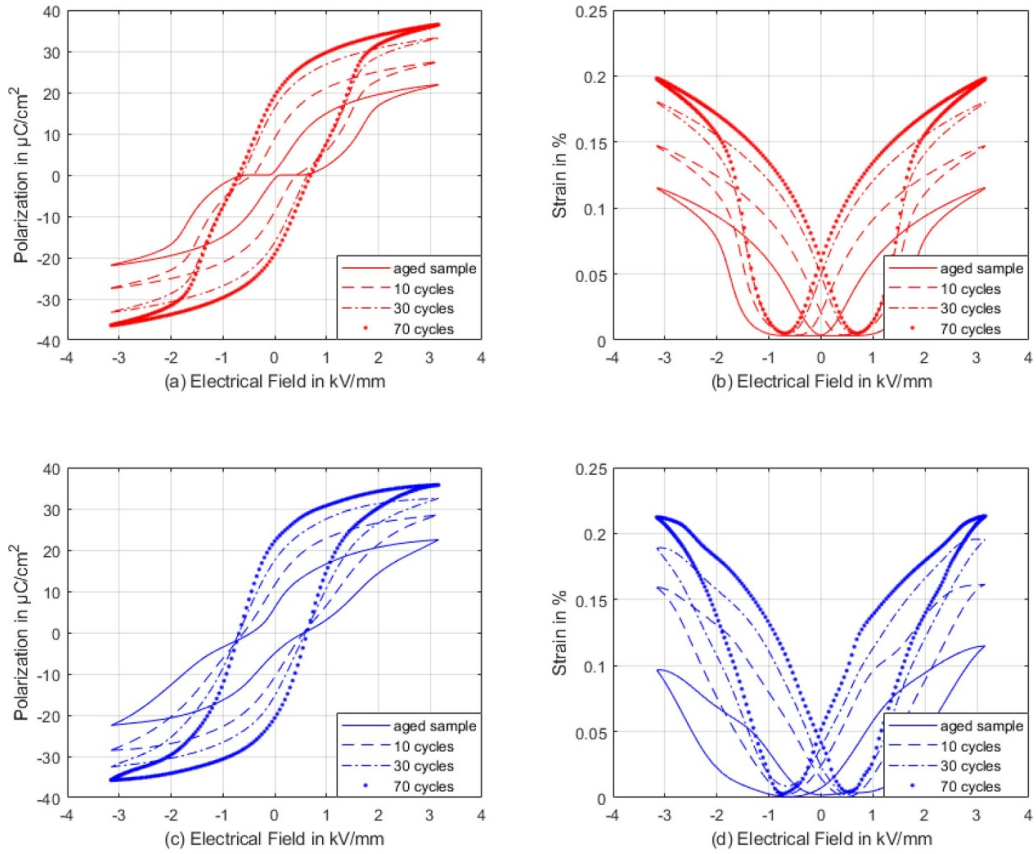

Figure 4. Hysteresis loops in the ageing simulation: (a) simulation value for polarization; (b) simulation value for strain; (c) measured polarization value; (d) measured strain value.

next section on de-ageing simulations. The effect of a specific ageing process over time will be studied in the section on de-ageing.

4.2. Simulation of de-ageing phenomenon

The experimental data used in this section was obtained for PZT:0.1Fe ceramics from [20]. According to [3, 21], the internal bias field is in an exp∼ format in the case of the de-ageing phenomenon:

$$E_{\text{internal}}(t) = ae^{-\frac{t}{b}} + c \tag{20}$$

Since $\xi(t)$ is a non-180° switching percentage variable and it is related to the internal bias field, we assume that it is consistent with the format of $E_{\text{internal}}(t)$ in order to simplify the calculation:

$$\xi(t) = de^{-\frac{t}{e}} + g \tag{21}$$

where *a, b, c, d, e* and *g* are the parameters that need to be identified. All the parameter identification works in the current paper can be completed by using the 'fmincon' function in Matlab.

In this part, the number of cycles of external field, which are called 'cycles' in the current paper, is applied instead of

seconds to represent the time functions related to the internal bias field and $\xi(t)$. Since the experimental sample is strictly pre-processed [20], it is assumed that the initial state is a fully aged sample. However, since the hysteresis curve remains almost unchanged after 70 cycles and no longer has the double hysteresis loop property, it can be considered to be the same as the fresh sample. To simplify the calculation, we assume that the 70 cycles are fresh sample, which means it has a zero internal bias field, and the 0 cycles are the fully aged sample. First, we simulate the fresh sample to determine the model coefficients, and perform new simulations at each subsequent stage to determine the value of the internal bias electrical field. The detailed strategy is presented as follows:

(a) Identify the initial values of the single-crystal parameters τ_p, a_2, a_4, a_6, τ_ε, k and b by using the 70 cycles sample data;
(b) Identify the initial values of the internal bias field variable $E_{\text{internal}}(t)$ and non-180° switching percentage variable $\xi(t)$ by using the 30 cycles, 10 cycles and 0 cycles sample data;
(c) The remaining strategy is the same as that used in the ageing part.

All the values can be referred to as table 2. The specific recognition results are shown in figure 4. Figures 4(a) and (c) show the hysteresis loops for the simulation and the measured polarization values, respectively. Figures 4(b) and (d) show the 'butterfly' loops of the simulation and the measured strain values, respectively. It can be seen from figure 4 that the model simulates the evolution trend for the ageing/de-ageing phenomenon very well. The new additional item can successfully simulate the ageing phenomena as proved by the above two numerical experiments.

However, it can also be found that the measured strain values in the figure are not completely symmetrical, but due to the assumption of the free energy function for our model before, the simulation diagrams are all symmetrical, which leads to a slight difference in the final simulation and measured values. This situation can be improved by upgrading the model to a 3D model, or by considering the addition of an asymmetric term to the free energy function of the model. For example, consider adding a new polarization-strain coupled term, such as 'εP' to improve the strain simulation value. Interested readers can try this for themselves.

5. Conclusion

In this paper, a phenomenological model on macroscopic level with a new free energy function was developed to describe the ageing hysteresis in ferroelectric ceramics. A new phenomenological term that combines an internal bias electrical field and polarization was proposed to simulate the ageing phenomenon. The new additional term ensures that the current model completes the hysteretic behaviour transformation from single loops to double loops. The current paper strongly proves this point based on numerical experiments for the ageing and de-ageing phenomena. The capability of the new term in the free energy function developed in the current model for characterizing the hysteretic phenomenon with ageing and de-ageing phenomena is verified.

Acknowledgment

This work has been supported by the National Natural Science Foundation of China (Grant No. 51575478 and Grant No. 61571007), the National Sciences and Engineering Research Council (NSERC) of Canada, and the Canada Research Chair Program. RM is also acknowledging support of the BERC 2018-2021 program and Spanish Ministry of Science, Innovation, and Universities through the Agencia Estatal de Investigacion (AEI) BCAM Severo Ochoa excellence accreditation SEV-2017-0718.

ORCID iDs

Xuan He https://orcid.org/0000-0002-4505-7700
Haoyuan Du https://orcid.org/0000-0001-8952-2355
Dan Wang https://orcid.org/0000-0003-0563-8030
Linxiang Wang https://orcid.org/0000-0002-7716-3794
Roderick Melnik https://orcid.org/0000-0002-1560-6684

References

[1] Ramesh R, Chan W K, Wilkens B, Sands T, Tarascon J M, Keramidas V G and Evans J T 1992 Fatigue and ageing in ferroelectric PbZr0.2Ti0.8O3/YBa2Cu3O7 heterostructures *Integr. Ferroelectr. Int. J.* **1** 1–15
[2] Damjanovic D 1998 Ferroelectric, dielectric and piezoelectric properties of ferroelectric thin films and ceramics *Rep. Prog. Phys.* **61** 1267
[3] Genenko Y A, Glaum J, Hoffmann M J and Albe K 2015 Mechanisms of ageing and fatigue in ferroelectrics *Mater. Sci. Eng.* B **192** 52–82
[4] Zhang L and Ren X 2006 Aging behavior in single-domain Mn-doped BaTiO3 crystals: implication for a unified microscopic explanation of ferroelectric ageing *Phys. Rev.* B **73** 094121
[5] Smith R C and Hom C L 1999 Domain wall theory for ferroelectric hysteresis *J. Intell. Mater. Syst. Struct.* **10** 195–213
[6] Rojac T, Kosec M, Budic B, Setter N and Damjanovic D 2010 Strong ferroelectric domain-wall pinning in BiFeO3 ceramics *J. Appl. Phys.* **108** 1315–465
[7] Yuan G L, Yang Y and Wing S 2007 Ageing-induced double ferroelectric hysteresis loops in BiFeO3 multiferroic ceramic *Appl. Phys. Lett.* **91** 122907
[8] Arlt G and Neumann H 1988 Internal bias in ferroelectric ceramics: origin and time dependence *Ferroelectrics* **87** 109–20
[9] Erhart P and Albe K 2008 Modeling the electrical conductivity in BaTiO3 on the basis of first-principles calculations *J. Appl. Phys.* **104** 044315–8
[10] Cockayne E and Burton B P 2004 Dipole moment of a Pb-O vacancy pair in PbTiO3 *Phys. Rev.* B **69** 144116
[11] Su Y and Landis C M 2015 Continuum thermodynamics of ferroelectric domain evolution: theory, finite element implementation, and application to domain wall pinning *J. Mech. Phys. Solids* **55** 280–305

[12] Schrade D, Mueller R, Xu B X and Gross D 2007 Domain wall pinning by point defects in ferroelectric materials *Proc. SPIE* **6526**: 65260B
[13] Wang L and Willatzen M 2007 Nonlinear dynamical model for hysteresis based on nonconvex potential energy *J. Eng. Mech.* **133** 506–13
[14] Wang L 2008 Hysteretic dynamics of ferroelectric materials under electro-mechanical loadings *Proceedings of the ASME 2008 Conference on Smart Materials, Adaptive Structures and Intelligent Systems. Smart Materials, Adaptive Structures and Intelligent Systems, Volume 1 October 28–30, 2008* (Ellicott City, Maryland, USA: ASME) 189–95
[15] Wang L and Melnik R 2009 Control of coupled hysteretic dynamics of ferroelectric materials with a Landau-type differential model and feedback linearization *Smart Mater. Struct.* **18** 074011
[16] Wang D, Wang L and Melnik R 2017 A hysteresis model for ferroelectric ceramics with mechanism for minor loops *Phys. Lett.* A **381** 344–50
[17] He X, Wang D, Wang L and Melnik R 2018 Modelling of creep hysteresis in ferroelectrics *Phil. Mag.* **98** 1256–71
[18] Feng Z and Ren X 2008 Striking similarity of ferroelectric ageing effect in tetragonal, orthorhombic and rhombohedral crystal structures *Phys. Rev.* B **77** 134115
[19] He X, Du H, Tong Z, Wang D and Melnik R 2020 A dynamic hysteresis model based on Landau phenomenological theory of fatigue phenomenon in ferroelectrics *Mater. Today Commun.* **25** 101479
[20] Glaum J, Genenko Y A, Kungl H, Schmitt L A and Granzow T 2012 De-ageing of fe-doped lead-zirconate-titanate ceramics by electric field cycling: 180°- vs. Non-180° domain wall processes *J. Appl. Phys.* **112** 903–15
[21] Carl K and Hardtl K H 1978 Electrical after-effects in Pb(Ti, Zr)O3 ceramics *Ferroelectrics* **17** 473–86